Relationship of Proton Uptake on the Cytoplasmic Surface and Reisomerization of the Retinal in the Bacteriorhodopsin Photocycle: An Attempt To Understand the Complex Kinetics of the pH Changes and the N and O Intermediates†

Yi Cao,‡ Leonid S. Brown,‡ Richard Needleman,§ and Janos K. Lanyi*,‡

Department of Physiology and Biophysics, University of California, Irvine, California 92717, and the Department of Biochemistry, Wayne State University School of Medicine, Detroit, Michigan 48201

Received May 14, 1993; Revised Manuscript Received July 19, 1993●

ABSTRACT: In the bacteriorhodopsin photocycle the recovery of the initial BR state from the M intermediate occurs via the N and O intermediates. The molecular events in this process include reprotonation of the Schiff base and the subsequent uptake of a proton from the cytoplasmic side, as well as reisomerization of the retinal from 13-cis to all-trans. We have studied the kinetics of the intermediates and the proton uptake. At moderately low pH little of the N state accumulates, and the O state dominates in the reactions that lead from M to BR. The proton uptake lags behind the formation of O, suggesting the sequence $N^{(0)} \leftrightarrow O^{(0)} + H^+$ (from the bulk) $\rightarrow O^{(+1)} \rightarrow BR + H^+$ (to the bulk), where the superscripts indicate the net protonation state of the protein relative to BR. Together with a parallel study of ours at moderately high pH, these results suggest that the sequence of proton uptake and retinal reisomerization depends on pH: at low pH the isomerization occurs first and O accumulates, but at high pH the isomerization is delayed and therefore N accumulates. Although this model contains too many rate constants for rigorous testing, we find that it will generate most of the characteristic pH-dependent kinetic features of the photocycle with few assumptions other than pH dependency for protonation at the proton release and uptake steps.

Absorption of light by the chromophore of the proton pump bacteriorhodopsin causes the all-trans to 13-cis isomerization of the retinal [recently reviewed in Mathies et al. (1991), Lanyi (1992), Oesterhelt et al. (1992), and Ebrey (1993)]. This photoreaction initiates a sequence of thermal reactions with an overall turnover time of about 10 ms under normal conditions, the "photocycle", in which recovery of the initial state is through the spectroscopically distinct intermediates[1] K, L, M, N, and O that arise and decay in the nanosecond to millisecond time range. Although for long a matter of controversy, according to a growing concensus (Gerwert et al., 1990; Ames & Mathies, 1990; Váró & Lanyi, 1991b; Lozier et al., 1922; Souvignier & Gerwert, 1992) most features of the photocycle can be described by a single sequence with many reversible reactions. Our version of this sequence was

$$BR \xrightarrow{h\nu} K \leftrightarrow L \leftrightarrow M_1 \rightarrow M_2 \leftrightarrow N \leftrightarrow O \rightarrow BR$$

(Váró & Lanyi, 1991b,c). These chromophore reactions are accompanied by proton transfers inside the protein and between the protein and the aqueous phase, arranged in a vectorial fashion so as to result in the net transport of a proton from the cytoplasmic to the extracellular side. Although the reactions of the chromophore are approximated by a linear sequence, the molecular events in the protein associated with them are more complex and depend on external influences such as the pH (Zimányi et al., 1992b, 1993). According to much evidence [summarized for example in Lanyi (1992) and Ebrey (1993)], the following occur near neutral pH: (1) in $L \rightarrow M_1$ the Schiff base proton is transferred to D85 located on the extracellular side of the Schiff base, (2) a proton is released to the bulk from an unidentified group that interacts with D85, termed XH (Zimányi et al., 1992b), (3) in $M_1 \rightarrow M_2$ access to the Schiff base changes from the extracellular to the cytoplasmic region of the protein (the reprotonation switch), (4) in $M_2 \rightarrow N$ the Schiff base is reprotonated from D96 located on the cytoplasmic side, (5) during the lifetime of N a proton is taken up from the bulk (Drachev et al., 1984; Zimányi et al., 1993) and D96 is reprotonated, (6) in $N \rightarrow O$ the retinal reisomerizes to all-trans, and (7) in $O \rightarrow BR$ the initial state of the protein is regained as D85 reprotonates the proton release group XH. We had found (Zimányi et al., 1992b) that at lower pH the sequence was somewhat different, because when the pH was below the pK_a for the proton release, XH remained protonated throughout the cycle and thus no proton could be released in step 2. Instead, the first proton exchange with the aqueous phase was the uptake in step 5, and proton release was delayed until step 7. This late proton release is probably directly from D85. We suggested, therefore, that, from the standpoint of those protonation reactions that involve protein residues rather than the Schiff base, the cycle after M_1 can proceed along two alternative pH-dependent pathways and in this sense its description as a single pathway is not quite accurate.

Absorbance changes of pH-indicator dyes in the bulk (Drachev et al., 1984; Grzesiek & Dencher, 1986; Heberle & Dencher, 1990, 1992; Otto et al., 1989, 1990; Zimányi et al.,

† This work was supported by grants to J.K.L. from the National Institutes of Health (GM 29498) and the Department of Energy (DEFG03-86ER13525) and to R.N. from the National Science Foundation (MCB-9202209), the U.S. Army (DAAL03-92-G-0406), and the Department of Energy (DEFG02-92ER20089).

* To whom correspondence should be addressed.

‡ University of California.

§ Wayne State University School of Medicine.

● Abstract published in *Advance ACS Abstracts*, September 1, 1993.

[1] Abbreviations: pyranine, 8-hydroxy-1,3,6-pyrenetrisulfonate; Bis-Tris-propane, 1,3-bis[[tris(hydroxymethyl)methyl]amino]propane. K, L, M, N, and O are the photointermediates of the bacteriorhodopsin photocycle; BR is the initial state. The early intermediates J and KL are omitted for simplicity. Superscripts, where given, refer to the net protonation of the protein relative to the initial state. Subscripts for M substates refer to pre- and postswitch states (M_1 and M_2; Váró & Lanyi, 1991b; Zimányi et al., 1992a).

0006-2960/93/0432-10239$04.00/0

1992b) near neutral pH detect release of a proton to the aqueous phase at about 400 μs and a subsequent uptake at 10–15 ms. A transient proton deficit develops therefore in the protein between these times. Dyes covalently bound at the surface detect the appearance of a proton at about 100 μs, i.e., roughly concurrently with the accumulation of the M state (Heberle & Dencher, 1992; Scherrer et al., 1992). According to calculations from the pH dependence of the rate constants, the proton release is to be placed just *after* the internal transfer of the Schiff base proton to D85 rather than concurrent with the proton transfer (Zimányi et al., 1992b). Thus, the L to M sequence could be resolved into either $L^{(0)} \leftrightarrow M_1^{(0)} \leftrightarrow M_1^{(-1)} + H^+$ (to the bulk) $\leftrightarrow M_2^{(-1)}$ or $L^{(0)} \leftrightarrow M_1^{(0)} \leftrightarrow M_2^{(0)} \leftrightarrow M_2^{(-1)} + H^+$ (to the bulk). Naturally, although represented as an equilibration, the reaction in which a proton is exchanged between the protein and the aqueous phase will appear to be reversible only near the pK_a for the release (calculated to be about 6). Additionally, the $M_1 \leftrightarrow M_2$ reaction (the reprotonation switch) was found to be strongly biased in the forward direction. We report elsewhere (Zimányi et al., 1993) that the proton uptake on the cytoplasmic side later in the cycle is also more complex than first suspected, and here the kinetics define in turn the pK_a for the proton uptake. At a pH high enough to ensure that the O state does not accumulate, proton uptake was detected after the rise of what difference spectra identified as N but before its decay. Thus, the relationship of proton kinetics to chromophore kinetics suggested temporal separation of the reisomerization of the retinal and the proton uptake. This resolved the M to N sequence at high pH into $M_2^{(-1)} \leftrightarrow N^{(-1)} + H^+$ (from the bulk) $\leftrightarrow N^{(0)}$. The first reaction is protonation equilibrium between the Schiff base and D96. The second reaction is proton uptake that occurs with a calculated pK_a of about 11. Since the retinal configuration in N is still 13-cis (Fodor et al., 1988), we had suggested that the decay of $N^{(0)}$ in the next step includes the reisomerization of the retinal and all other events which regenerate the initial state.

Below the pK_a of the proton release group (e.g., at pH 4 or 5) the absorbance changes of pH-indicator dyes (Dencher & Wilms, 1975; Zimányi et al., 1992b) showed that the early proton release is absent. The sequence of pH changes is therefore reversed: first a proton is taken up in the several millisecond time range as occurs at higher pH, and this is followed by proton release as BR recovers from O at the end of the photocycle. The transient net gain of proton was suggested to correlate therefore with the O state. However, the temporal sequences of proton uptake and retinal reisomerization have not been investigated under these conditions. In general, the accumulation of the O state and its pH dependent relationship to the M and N states have been one of the problems in the photocycle. Recent results indicate that the reason for the much greater accumulation of O at low pH than at high pH (Lozier et al., 1978; Li et al., 1984; Ames & Mathies, 1990) cannot be the pH dependence of the rise or the decay. In the relevant pH region (between 6 and 8) these time constants (in the millisecond range) are not very pH dependent (Ohtani et al., 1992; Eisfeld & Stockburger, 1992). One of the possible explanations is that there is a rapid pH-dependent equilibrium between N and O (Chernavskii et al., 1989; Souvignier & Gerwert, 1992), and thus the rise of O occurs with the (pH-independent) time constant of the M to N reaction. However, this cannot be the entire explanation because in most studies the rise of O is found to be somewhat delayed relative to the rise of N, suggesting that the $N \leftrightarrow O$ equilibration is not instantaneous relative to the rise of N. The rate of the reequilibration of O after a temperature jump applied to bacteriorhodopsin films was rapid enough to suggest that the time constant of the $N \leftrightarrow O$ equilibrium is as short as 100 μs (Chernavskii et al., 1989), but in similar temperature-jump experiments with aqueous membrane suspensions the reequilibration rate was much slower (Chizhov et al., 1992). According to time-resolved resonance Raman (Ames & Mathies, 1990) and absorption spectroscopy in the visible (Váró & Lanyi, 1991b), the N to O time constant near neutral pH was either somewhat slower or roughly the same as that of the M to N reaction. According to a study with time-resolved FTIR (Souvignier & Gerwert, 1992), the N to O reaction was faster, but not considerably, than the M to N reaction. A possible explanation is a shunt from N to BR (Váró et al., 1990). Alternatively, it has been suggested (Dancsházy et al., 1988; Eisfeld & Stockburger, 1992) that there are parallel photocycles originating from two or more pH-dependent bacteriorhodopsin subpopulations, and one of the photocycles contains O but not N and the other contains N but not O.

In this study we measured proton uptake by transient absorption changes of the pH-indicator dye pyranine. The retinal isomerization was conveniently followed by the $N \rightarrow O$ chromophore transition because these intermediates absorb at widely separated wavelengths.[2] The results provide additional support for the pH-dependent branched model proposed recently (Zimányi et al., 1992b). In an attempt to refine the model we explored the relationship of the proton uptake from the cytoplasmic surface and the reisomerization of the retinal from 13-cis to all-trans, i.e., the events revealed by the kinetics of the N and O intermediates. Particular emphasis was given in these studies to the relationship of the proton uptake process to the formation of the O state. We found that, in contrast with the findings at high pH where proton uptake was *before* retinal reisomerization (Zimányi et al., 1993), proton uptake at low pH takes place *after* the reisomerization. Analogously to the two N states at high pH, this requires the existence of two O states and resolves the N to BR reaction at low pH into $N^{(0)} \leftrightarrow O^{(0)} + H^+$ (from the bulk) $\rightarrow O^{(+1)} \rightarrow BR + H^+$ (to the bulk). We suggest that, for the same reason that little of the O state accumulates at high pH, little of the N state accumulates at low pH.

MATERIALS AND METHODS

Recombinant *bop* genes with the R82Q, R82A, or L93T residue replacements were introduced into *Halobacterium halobium* with a shuttle vector described before (Ni et al., 1990; Needleman et al., 1991). Purple membranes containing these or the wild-type protein were purified by a standard method (Oesterhelt & Stoeckenius, 1974). All sample preparation and spectroscopy were as described elsewhere (Cao et al., 1993), except that photoexcitation was with a

[2] This is based on the fact that N and O contain 13-*cis*- and *all-trans*-retinal, respectively (Fodor et al., 1988; Smith et al., 1983). According to numerous observations (Mogi et al., 1988; Holz et al., 1989; Butt et al. 1989; Stern et al., 1989; Miller & Oesterhelt, 1990; Thorgeirsson et al., 1991; Zimányi et al., 1993) the charge state of D96 or replacement of D96 has little or no effect on the absorption maximum of the chromophore in the unphotolyzed protein or N in the photocycle. The large red shift that characterizes the N to O transition is therefore attributed not to the proton uptake on the cytoplasmic side but to an altered Schiff base–counterion relationship as the Schiff base is displaced upon the 13-cis to all-trans isomerization. As expected from this, a red shift of similar magnitude exists between unphotolyzed 13-cis and all-trans acid blue bacteriorhodopsins where D85 is protonated as in N and O (Ohtani et al., 1986).

Ne-Yag laser (532 nm, 7-ns pulse length) and signal acquisition was with a Thurlby Model DSA 524 averager. Random noise was removed from the time-resolved difference spectra with SVD filtering as before. Kinetics were generated from rate constants with the program SIMULATE, written by L. Zimányi; fitting of time-dependent concentrations to exponentials and SVD analysis were with SPSERV, written by Cs. Bagyinka.

For the single wavelength measurements we chose wavelengths that were best suited to follow the photointermediates of interest. For M and N these wavelengths were 410 and 570 nm, respectively. For the O state the best wavelength was not at its probable maximum. In the wild type we used 700 nm where the absorption amplitude of BR is negligible. Although BR does absorb at 660 nm, we used this wavelength in the R82Q mutant because the amount of O was so small that it could not be detected at 700 nm. In the L93T mutant 540 and 640 nm were suitable wavelengths for N and O, respectively, because the maximum of this chromophore is strongly blue-shifted. The pH change kinetics during the photocycle were followed with pyranine as before (Cao et al., 1993). Where the temperature is not indicated, it was regulated at 22 °C.

RESULTS

Interconversions of the M, N, and O Intermediates of the Photocycle at Moderately Low pH. The N intermediate represents the chromophore after reprotonation of the Schiff base by D96 but before reisomerization of the retinal from 13-cis to all-trans (Fodor et al., 1988), while the O state represents the all-trans chromophore (Smith et al., 1983) before deprotonation of D85. Near neutral pH both N and O accumulate in the photocycle. It is well documented, however, that at pH above 8 or 9 the O state does not accumulate significantly and the N state accumulates in correspondingly greater amounts (Li et al., 1984; Lozier et al., 1978; Váró & Lanyi, 1990; Ames & Mathies, 1990; Ohtani et al., 1992). At pH below 6 it is the O state that accumulates in large amounts, but there is little information on N under these conditions. Although for mechanistic reasons we should assume that the N intermediate is produced also at low pH, we have suspected that for kinetic reasons it accumulates in much lesser amounts than at higher pH. This possibility was explored in the wild-type and the recombinant L93T proteins. The latter was expected to be a useful additional system in investigations of the O intermediate because in an earlier report of this mutant (Subramaniam et al., 1991) the O state was found to be produced in larger amounts and with kinetics greatly different from those of the wild type.

Panels A and B of Figure 1 show light-induced absorbance changes of wild-type and L93T bacteriorhodopsins, respectively, at pH 4. Global analysis of the changes at 410, 700 or 640, and 570 or 540 nm indicated that in the wild-type protein the rise of O has the same time constant (2.6 ms) as the faster of the two detectable decay components of M and its decay time constant (5.5 ms) is the same as those of the slower M decay component and the recovery of the initial state at 570 nm. In a linear sequence this kind of kinetics would suggest that M and O (and therefore N, if any) equilibrate through back-reactions and the equilibrium mixture decays to BR as suggested before (Chernavskii et al., 1989; Gerwert et al., 1990; Ames & Mathies, 1990; Váró & Lanyi, 1991b; Souvignier & Gerwert, 1992). In L93T (Figure 1B) the relationship of O to M is considerably changed. The rise of O has the same time constant as the decay of M (51 ms),

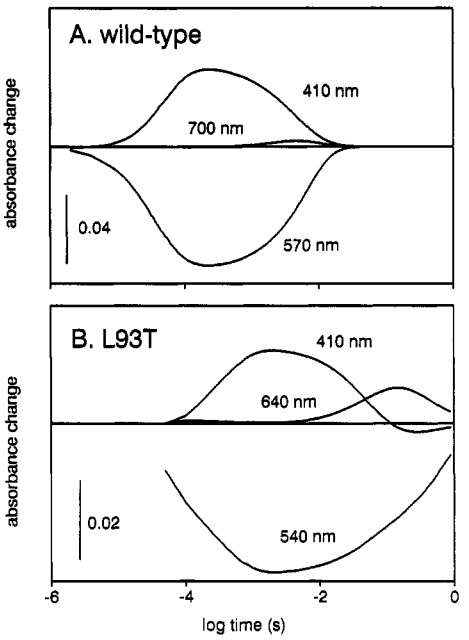

FIGURE 1: Absorbance changes in the photocycles of wild-type (A) and L93T (B) bacteriorhodopsins at moderately low pH. Conditions: 20 μM wild-type or 28 μM L93T bacteriorhodopsin, 100 mM NaCl, 20 mM sodium succinate, pH 4.0, and 35 °C.

but M decays virtually completely as O reaches its maximal amplitude, suggesting a unidirectional step in the M to O pathway. Since M and O are separated in time, the biphasic absorbance change at 540 nm contains the time constants for the decay of both. The O state decays and BR recovers with a common time constant of 670 ms. In this mutant, therefore, the rise of O is limited by a greatly slowed M decay, but O accumulates in larger amounts than in wild type in spite of this because the decay of O is slowed to an even greater extent. If there is N, it must be in rapid equilibrium with O (cf. below). The changed rates of the chromophore reactions indicate that the L93T residue substitution inhibits the transfer of a proton from D96 to the Schiff base (M → N) by 1 order of magnitude and the release of a proton from D85 (O → BR) by 2 orders of magnitude.

Figures 2 and 3 show measured time-resolved difference spectra for wild-type and L93T bacteriorhodopsins under the same conditions as in Figure 1. The strong blue shift of the depletion band of L93T in Figure 3A (541 vs 568 nm in wild type) is consistent with the blue-shifted maximum of the unphotolyzed chromophore of the mutant (540 vs 568 nm in wild type). The spectral transformations at wavelengths ≥600 nm in the microsecond time range reveal that the K state decays much more rapidly in L93T than in wild type while the changes in the millisecond time range confirm the greater accumulation of O, both as found before (Subramaniam et al. 1991). Since L93T contains little, if any, 13-cis–syn chromophore (Subramaniam et al., 1991), we do not expect that the red-shifted intermediate of the 13-cis photocycle contributed to these spectra. While the presence of N in the L93T photocycle at pH 6 was suggested by resonance Raman (Subramaniam et al., 1991), its amount at low pH is not simple to decide in either this or the wild-type photocycle.

In analyzing these spectra, we have taken advantage of the earlier finding (Zimányi et al., 1992b) that at pH <6 the intermediates K, L, and M come to an equilibrium and decay with a constant concentration ratio. Thus, we subtracted an appropriately scaled difference spectrum from the time where

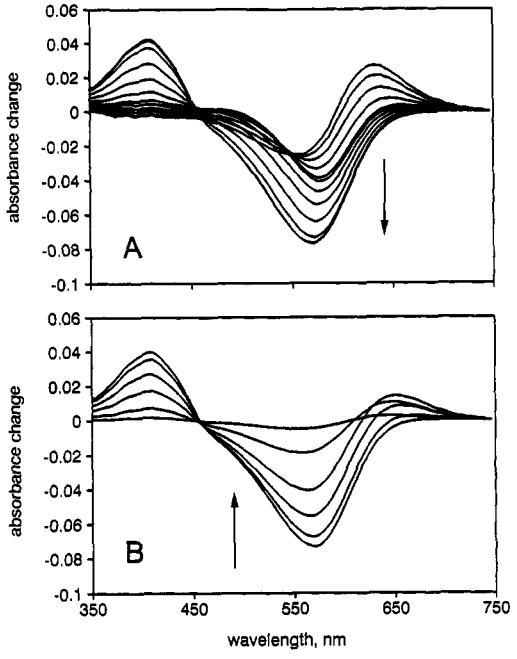

FIGURE 2: Time-resolved difference spectra for wild-type bacteriorhodopsin at moderately low pH. Conditions as in Figure 1. Delay times after photoexcitation: (A) 70 ns, 150 ns, 310 ns, 650 ns, 1.4 μs, 2.9 μs, 6 μs, 13 μs, 27 μs, 56 μs, 120 μs, and 250 μs; (B) 520 μs, 1.1 ms, 2.3 ms, 4.9 ms, 10 ms, and 21 ms.

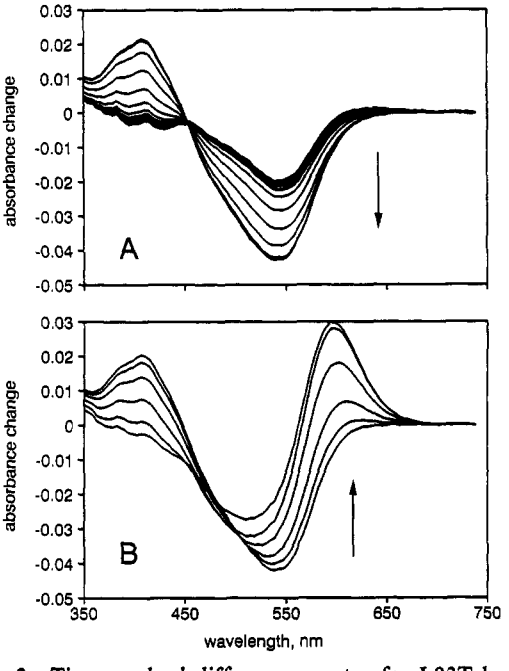

FIGURE 3: Time-resolved difference spectra for L93T bacteriorhodopsin at moderately low pH. Conditions as in Figure 1. Delay times after photoexcitation: (A) 70 ns, 150 ns, 310 ns, 650 ns, 1.4 μs, 2.9 μs, 6 μs, 13 μs, 27 μs, 56 μs, 120 μs, 250 μs, 520 μs, 1.1 ms, and 2.3 ms; (B) 4.9 ms, 10 ms, 21 ms, 45 ms, 94 ms, and 200 ms.

the maximal concentration of M was reached (where the K ↔ L ↔ M equilibration was assumed to have occurred already but little, if any, N was yet formed) from all subsequent spectra so as to eliminate absorbance change at 380–400 nm where only M has extinction significantly different from BR. The resulting net difference spectra for wild-type and L93T are shown in Figures 4 and 5, respectively, with their rising and falling phases in separate panels. In the wild type the initial spectra have untypical shapes but evolve quickly into what can be regarded as nearly pure O *minus* BR difference spectra

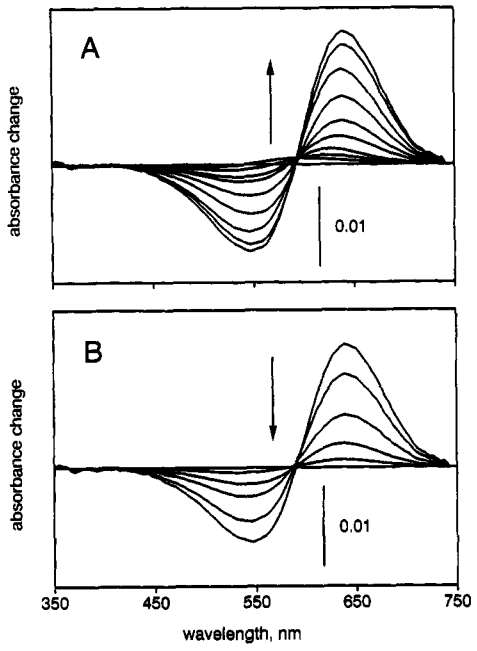

FIGURE 4: Net difference spectra for the second half of the wild-type photocycle. The difference spectrum at 170 μs was so scaled and subtracted from all subsequent difference spectra in Figure 2 that the absorbance change at 380–400 nm vanished. Delay times after photoexcitation: 250 μs, 360 μs, 520 μs, 760 μs, 1.1 ms, 1.6 ms, 2.3 ms, 3.3. ms, and 4.9 ms; (B) 7 ms, 10 ms, 15 ms, 21 ms, and 31 ms.

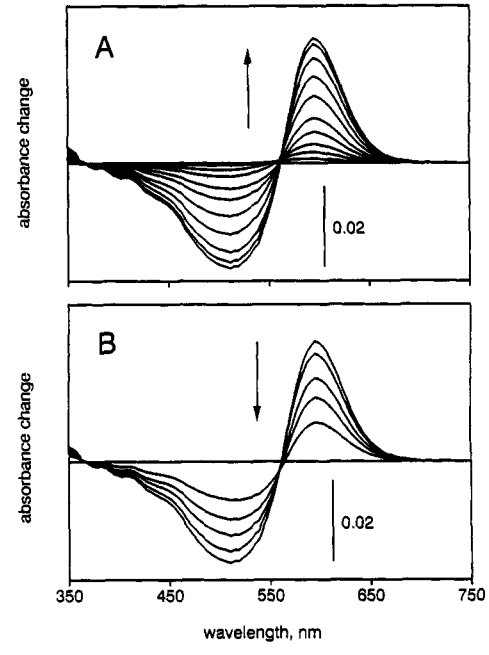

FIGURE 5: Net difference spectra for the second half of the L93T photocycle. The difference spectrum at 3.3 ms was so scaled and subtracted from all subsequent difference spectra in Figure 3 that the absorbance change at 380–400 nm vanished. Delay times after photoexcitation: (A) 4.9 ms, 7 ms, 10 ms, 15 ms, 21 ms, 31 ms, 45 ms, 65 ms, 94 ms, and 140 ms; (B) 200 ms, 290 ms, 420 ms, 600 ms, and 880 ms.

(Figure 4). They decrease nearly unchanged as BR recovers. Earlier estimations of the spectrum of O (Chernavskii et al., 1989; Váró & Lanyi, 1991a,c) gave difference maxima near 620–650 nm and asymmetrical shapes as would be expected from a difference spectrum between a red-shifted BR-like species and BR. The amplitudes of the difference maxima were 1.45–1.55 × greater than the minima. In the spectra for wild type (Figure 4) we find that the maximum is at 640 nm and the amplitude ratio is 1.52. Significant amounts of N in

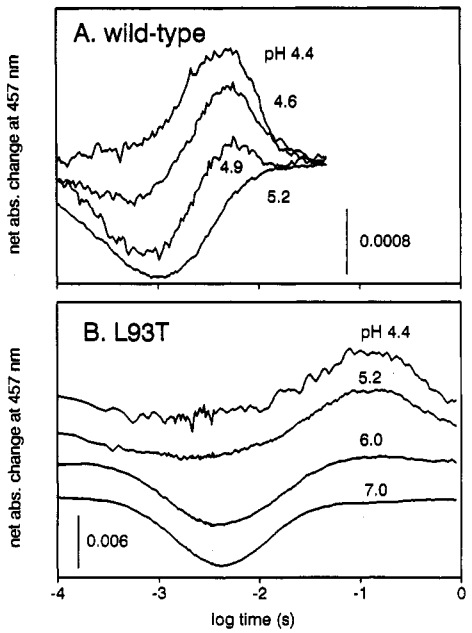

FIGURE 6: pH dependence of proton uptake and release in the photocycles of wild-type (A) and L93T (B) bacteriorhodopsins. The absorbance changes shown are for pyranine with buffered controls subtracted to eliminate contribution from the chromophore as before (Cao et al., 1993). Upward deflection is proton uptake. Conditions: 20 μM wild-type or 28 μM L93T bacteriorhodopsin, 2 M NaCl, and 0.1–1 mM pyranine. The buffer was sodium succinate; its final concentration was 20 mM. The traces are scaled to the same amplitude.

the equilibrium mixture would have added negative amplitude to the depletion band and decreased this ratio. Somewhat similar difference spectra were obtained in L93T (Figure 5). The maxima of the positive and negative bands are both strongly blue-shifted relative to the wild type, consistent with the blue-shifted maximum of the unphotolyzed L93T. The amplitude ratio is 1.2, however, suggesting the presence of N. Since the shape of these spectra changes only slightly with time, the concentration ratio of N to O appears to remain constant as BR recovers. The presence of N in these spectra is suggested additionally by the fine structure observed between 350 and 400 nm (Figure 5), such as found at higher pH for N *minus* BR spectra (Dancsházy et al., 1988; Fukuda & Kouyama, 1992; Zimányi et al., 1993). By the same token, this fine structure is largely absent in the spectra for wild type (Figure 4). We conclude from these spectral decompositions that the N intermediate does not accumulate significantly in the wild type photocycle, but the same criteria that rule out N in the wild type allow some of the N intermediate to accumulate in the L93T photocycle and indicate that it is in equilibrium with O.

Changed Proton Kinetics at Low pH. The reversal of the order of proton release and uptake at low pH had been detected with bromocresol green (Dencher & Wilms, 1975) and chlorophenol red (Zimányi et al., 1992b) as pH-indicator dyes. We repeated these experiments with the more commonly used dye pyranine, as its large negative charge precludes binding to the protein and therefore the possibility that its absorbance changes might be influenced by surface effects. Since protein residues strongly buffer at pH <6, and the pH range of interest extends well below the pK_a of pyranine, these experiments required the use of high pyranine concentrations and the exercise of great care to detect the small net signals from the dye. Panels A and B of Figure 6 show the proton kinetics measured in wild type and L93T, respectively, between pH 4 and pH 7. Although with greatly different rise and decay time constants for the pH changes, as expected from the chromophore kinetics in panels A and B of Figure 1, the basic elements of the model are confirmed in both of these systems. At higher pH proton release precedes uptake resulting in *net release* in the cycle, but as the pH is decreased this pattern is replaced by another in which uptake precedes release and there is *net uptake* at a later time in the cycle. Because in the wild-type protein at low pH the uptake and release follow each other very closely in time, the amplitude and shape of the traces are strongly influenced by small changes in the formation and decay rates. For the same reason the absorbance changes are considerably smaller than in L93T where the kinetics are more favorable for measuring these effects. Thus, the more robust results with L93T in Figure 6B constitute important additional evidence to those with wild type in support of the earlier described pH dependent pattern of the proton kinetics. The results in Figure 6 strongly suggest also that in the pH range between net release and uptake (e.g., pH 4.6–4.9 in wild type or pH 5.2 in L93T) the photocycle must proceed along two alternative courses because on mechanistic grounds it is highly unlikely that there would be first proton release, then proton uptake, and then a second proton release in a single reaction sequence.

Relationship of the O Intermediate to Proton Uptake. As discussed before (Zimányi et al., 1992b), results such as in Figure 6 suggest that at low pH the uptake and the subsequent release of the proton might correlate with the accumulation and decay of the O intermediate. This aspect of the model is now tested directly by comparing the proton kinetics as measured with pyranine and the accumulation of O as measured by absorption rise in the red where in the millisecond time range absorption increase originates mostly or entirely from the O state.

Replacing R82 with a nonprotonatable residue renders the normal proton release mechanism nonfunctional (Otto et al., 1990; Balashov et al., 1992), and proton release on the extracellular membrane side is delayed until after proton uptake at any pH, in a manner similar to that at low pH in the wild type photocycle. Panels A and B of Figure 7 show absorbance changes at 660 nm (positive absorbance change is production of O; negative change is depletion of BR) and net absorbance changes at 457 nm due to pyranine (increase is proton uptake), respectively, after photoexcitation of R82Q. The measurements were at 35, 20, and 5 °C, under conditions where D85 is mostly deprotonated, i.e., where the purple form of the unphotolyzed chromophore predominates. Since the O intermediate is unique in the photocycle in that its accumulation increases with increasing temperature (Hoffmann et al., 1978; Sherman et al., 1979; Lozier et al., 1984; Li et al., 1984; Chernavskii et al., 1989; Váró & Lanyi, 1991b; Chizhov et al., 1992), the temperature dependence of the amplitude of the proton uptake constitutes a test of the relationship of O and the protonation reaction. As expected, the formation of some O is evident from the absorption increase at 5–6 ms at 35 °C, but less is produced at about 10 ms at 20 °C and much less (although not necessarily none) is seen at 5 °C (Figure 7A). In contrast, the amount of protons taken up is not strongly dependent on temperature (Figure 7B). It is evident that the accumulation of O and the proton uptake are roughly correlated in time but not in amplitude. This makes it doubtful that there is a one-to-one relationship between them.

Comparison of the 35 °C traces in panels A and B of Figure 7 suggests that the maximal accumulation of O might occur

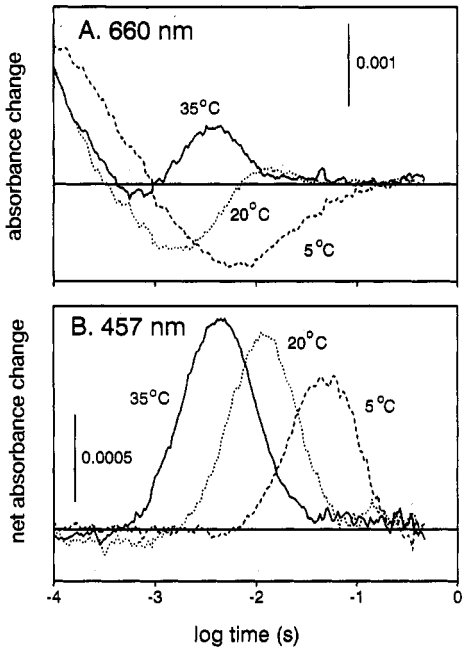

FIGURE 7: Comparison of the kinetics of the O state (followed at 660 nm, A) with the kinetics of proton uptake (followed at 457 nm with pyranine, B) in R82Q bacteriorhodopsin. Conditions: 20 μM R82Q bacteriorhodopsin, pH 7.5, and otherwise as in Figure 6. The temperature was as indicated: 35 °C, solid lines; 20 °C, dotted lines; 5 °C, dashed lines.

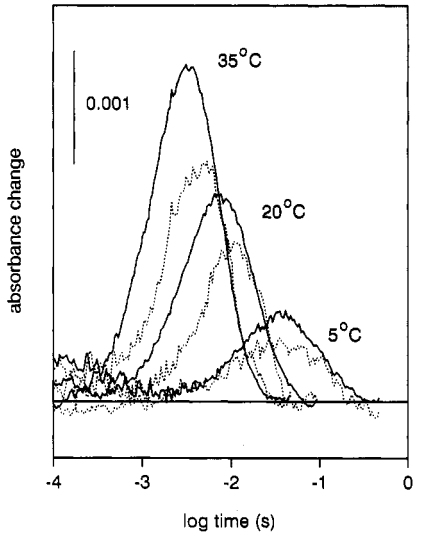

FIGURE 8: Comparison of the kinetics of the O state (followed at 700 nm, solid lines) with the kinetics of proton uptake (followed at 457 nm with pyranine, dotted lines) in wild-type bacteriorhodopsin. The temperatures were as indicated. Conditions as in Figure 7 but with wild-type protein and at pH 4.4.

somewhat earlier than the maximal proton uptake. This possibility was examined more closely in the wild-type system, where a greater amount of O accumulates but the pH of the measurement must be much lower to assure net proton uptake (Figure 6). Figure 8 shows O kinetics, measured at 700 nm (solid lines), and pH-change kinetics, measured with pyranine (dotted lines), at pH 4.4 at 5, 20, and 35 °C. Under these conditions virtually all of the chromophore is in the purple form. At the two higher temperatures the signal/noise is sufficient to indicate that the concentration of O reaches the maximum earlier than the proton uptake. Because these are noisy traces and the rise and decay processes are not well separated in time, their analysis as sums of rising and falling exponential processes is not unambiguous. Either the proton uptake is delayed relative to the rise of the O state or the proton release is delayed relative to the decay of O. The latter is not reasonable: that the proton release is coincident with the decay of O is supported by the fact that the absorption change at 570 nm (and therefore the recovery of the initial BR state) coincides with the decay of O (Figure 1). This is as expected from the generally held view that O is the last intermediate of the photocycle. Moreover, if the proton release occurred *after* the O → BR chromophore reaction, the deprotonation of D85 would occur without effect on the absorption maximum, contrary to the findings that this residue is the main component of the Schiff base counterion (Subramaniam et al., 1990, 1992; Needleman et al., 1991; Lanyi et al., 1992). According to the former alternative, where the proton uptake occurs during the O state, the absorption maximum of O would have to be unaffected by the protonation event on the cytoplasmic side, but this is reasonable because the proton acceptor D96 is about 12 Å removed from the Schiff base (Henderson et al., 1990). Thus, a fair interpretation of the results in Figure 8 is that proton uptake is delayed relative to the formation of O. This delay at 20 °C is about 3 ms, i.e., much longer than the time constant of 0.4–0.5 ms for detecting protons in the bulk with pyranine after their release on the extracellular side at higher pH (cf. Figure 6, for example). Although the net charge densities of the two membrane surfaces are not quite equal (Scherrer et al., 1992), it seems very unlikely that under the conditions used (low pH, high salt concentration) the bulk to surface proton equilibration would have a significantly longer time constant on the cytoplasmic side. The results suggest instead that the retinal reisomerization and the proton uptake are not concurrent.

As a control, we examined the relationship of proton uptake and O rise kinetics in L93T where O is produced on a longer time scale and concurrently with M decay (Figure 1B). In this system the proton uptake will not necessarily lag behind the rise of O because the rate of M decay is so much slower than in wild type that it is likely to limit the subsequent reactions, i.e., both the formation of O and the proton uptake (Figure 1B). Indeed, analysis of the spectra during and after M decay suggested that in this protein N and O reach an equilibrium already during the formation of O (Figure 5). The subsequent proton release may be expected to coincide with the decay of O as in wild type. Figure 9 shows data with the L93T protein at pH 4.4 and 35 °C. In this system the proton uptake and release do coincide with the rise and decay of O.

The results thus indicate that at pH <5 in the wild-type protein proton uptake is delayed relative to the rise of O, in much the same way it was delayed relative to the rise of N at pH >9 (Zimányi et al., 1993). Thus, in an analogous manner to the two sequential N states at high pH, we postulate the occurrence of two sequential O states at low pH. The first O is designated as $O^{(0)}$ because its protonation state is the same as BR and the second as $O^{(+1)}$ because it represents the gain of a proton. We describe, therefore, the low-pH pathway from N to BR by the scheme $N^{(0)} \leftrightarrow O^{(0)} + H^+$ (from the bulk) $\leftrightarrow O^{(+1)} \rightarrow BR + H^+$ (to the bulk). This sequence, together with the complementary scheme for high pH suggested elsewhere (Zimányi et al., 1993), is summarized in Figure 10. It should be noted that the separation of the proton uptake step from the retinal reisomerization step emphasized in this scheme was recognized, at least conceptually, in earlier reports already [e.g., Mathies et al. (1991)].

Comparing the pH Dependence of the Measured Time Constants for M and O with Those Generated by the Model.

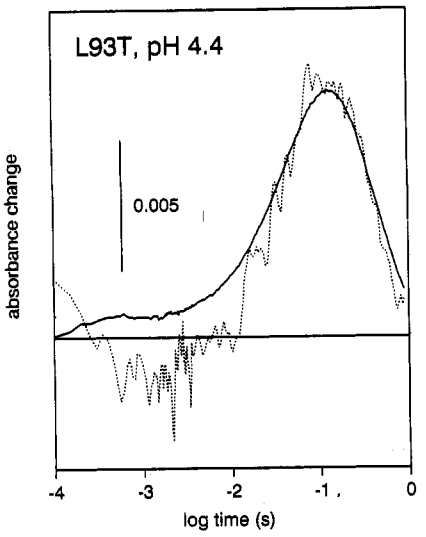

FIGURE 9: Comparison of the kinetics of the O state (followed at 640 nm, solid line) with the kinetics of proton uptake (followed at 457 nm with pyranine, dotted line) in L93T bacteriorhodopsin. Conditions: 28 μM L93T bacteriorhodopsin, 35 °C, and otherwise as in Figure 7.

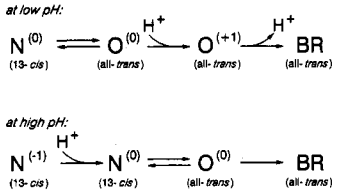

FIGURE 10: Proposed sequence of chromophore and proton transfer reactions in the photocycle at low pH (e.g., <5) and high pH (e.g., >8). The reisomerization of the retinal from 13-cis to all-trans is before proton uptake at low pH but afterward at high pH. The consequence of this is that both O and N states are resolved into two sequential substates, the first occurring before and the second after the proton uptake.

It was pointed out recently that several processes in the photocycle have nontrivial pH dependencies that are not likely to have simple explanations (Eisfeld & Stockburger, 1992). The most striking effects pertain to the amplitudes and time constants of two principal M decay components and of the decay of O. These intermediates are the easiest to follow because in wild-type all-trans BR their rise and decay kinetics can be determined unambiguously from absorbance changes at 410 and 700 nm, respectively (cf. above). Although it is well-known that at pH above 8 the slower M decay component becomes progressively slower with increasing pH [e.g., Groma et al. (1984), Otto et al. (1989), Váró & Lanyi (1990), Cao et al. (1991), Kouyama et al. (1988), and Zimányi et al. (1993)], it is not generally recognized that its amplitude declines with increasing pH [as discussed by Otto et al. (1989)]. The decay of O also becomes slower in this pH region, while its rise remains fairly pH independent. At the same time the amplitude of O strongly declines with increasing pH above pH 6 (Lozier et al., 1978; Li et al., 1984; Váró & Lanyi, 1991b; Eisfeld & Stockburger, 1992). We have repeated the measurements of the kinetics of M and O. The absorbance changes at 410 and 700 nm between pH 4 and pH 10 were analyzed as sums of exponentials, and the amplitudes and time constants are shown in Figure 11. They confirm the results of Eisfeld and Stockburger (1992).

Would a model that incorporates the pathways in Figure 10 be consistent with these kinetic features? There are two main alternatives that are not necessarily mutually exclusive. In the first, the pH dependence of the amplitude of O originates

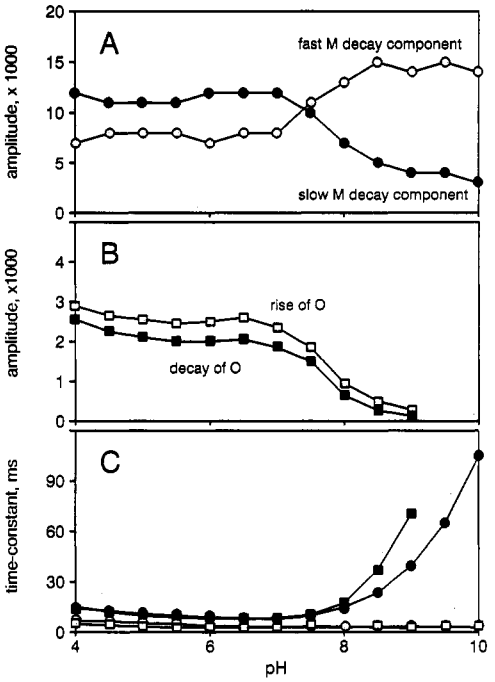

FIGURE 11: pH dependence of the decay kinetics for M and rise and decay kinetics for O in wild-type bacteriorhodopsin. Absorbance changes were measured at 410 and 700 nm (for M and O, respectively) between 0.1 ms and 1 s after photoexcitation, and exponentials were fitted to the traces. (A) Amplitudes (in absorbance) for the faster (○) and the slower (●) decay components of M. (B) Amplitudes (in absorbance) for the rise (□) and decay (■) of O. The difference between the rise and decay amplitudes originates from a small negative amplitude at the beginning of the rise kinetics. (C) Time constants for the processes in (A) and (B). Because above pH 8 the amplitude of O is very small, the time constants for its decay are inaccurate, and the differences from the slower time constant of M decay may not be significant. Conditions: 20 μM bacteriorhodopsin, 100 mM NaCl, and sodium aspartate–sodium succinate–Bis-Tris-propane buffer, 20 mM each.

from the more rapid $O^{(0)} + H^+ \rightarrow O^{(+1)}$ reaction at low pH (that favors accumulation of $O^{(+1)}$ but not $O^{(0)}$ and $N^{(0)}$) and the less rapid $N^{(-1)} + H^+ \rightarrow N^{(0)}$ reaction at high pH (that favors accumulation of $N^{(-1)}$ but not $N^{(0)}$ and $O^{(0)}$); i.e., the amplitude of O is influenced by the rate of proton uptake. In the second, the pH dependence of the amplitude of O originates from a difference of the rate of retinal reisomerization in the two pathways shown in Figure 10; i.e., the amplitude of O depends on which pathway is taken, and it is determined therefore by the pK_a for proton release. This alternative requires that the low-pH pathway accumulate little N and the high-pH pathway accumulate little O. Although a clear decision between the two models cannot be made as yet, and the kinetics might well contain aspects of both, we tested the second as an intriguing and novel possibility suggested by the results in the present work. Figure 12 shows such a model, simplified so as to neglect the accumulation of N in the low pH branch and the accumulation of O in the high-pH branch (shown with brackets to emphasize this point). Even with this simplification, however, the model is too complex to be rigorously tested against data. For this reason, we reversed the usual procedure in which the model would be fitted to the measured data. Instead, we made some assumptions about which rate constants are likely to be pH dependent and generated photocycle kinetics from the model between pH 4 and pH 10. The kinetics calculated on this basis were then treated as if they were data, and its pH dependent features were compared with those of the measured data.

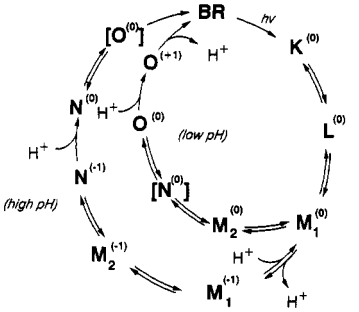

FIGURE 12: Model for the bacteriorhodopsin photocycle, based on results in this report and in earlier publications (Zimányi et al., 1992b, 1993). The N state at low pH and the O state at high pH are in brackets because they do not accumulate significantly under these conditions. They are left out of the kinetic simulation based on this model. The $M_1^{(0)} \leftrightarrow M_1^{(-1)} + H^+$ reaction is shown as in principle reversible because its pK_a is within the physiological range, while the $N^{(-1)} + H^+ \rightarrow N^{(0)}$ and $O^{(0)} + H^+ \rightarrow O^{(+1)}$ reactions are shown as unidirectional because their pK_a's are well above any pH likely to be encountered in vivo.

Table I: Input Rate Constants for Calculating the Kinetics of M and O from the Photocycle Model Shown in Figure 12[a]

reaction	pH 4	pH 6	pH 8	pH 10
$L \rightarrow M_1^{(0)}$	5×10^4	5×10^4	5×10^4	5×10^4
$M_1^{(0)} \rightarrow L$	1.25×10^5	1.25×10^5	1.25×10^5	1.25×10^5
$M_1^{(0)} \rightarrow M_2^{(0)}$	1.25×10^4	1.25×10^4	1.25×10^4	1.25×10^4
$M_2^{(0)} \rightarrow M_1^{(0)}$	625	625	625	625
$M_2^{(0)} \rightarrow O^{(0)}$	250	250	250	250
$O^{(0)} \rightarrow M_2^{(0)}$	100	100	100	100
$O^{(0)} \rightarrow O^{(+1)}$	250	250	67	5
$O^{(+1)} \rightarrow BR$	167	167	167	167
$M_1^{(0)} \rightarrow M_1^{(-1)}$	1.0×10^6	1.0×10^6	1.0×10^6	1.0×10^6
$M_1^{(-1)} \rightarrow M_1^{(0)}$	2.5×10^8	6.3×10^6	1.6×10^5	4.0×10^3
$M_1^{(-1)} \rightarrow M_2^{(-1)}$	1.25×10^4	1.25×10^4	1.25×10^4	1.25×10^4
$M_2^{(-1)} \rightarrow M_1^{(-1)}$	625	625	625	625
$M_2^{(-1)} \rightarrow N^{(-1)}$	250	250	250	250
$N^{(-1)} \rightarrow M_2^{(-1)}$	100	100	100	100
$N^{(-1)} \rightarrow N^{(0)}$	250	250	67	5
$N^{(0)} \rightarrow BR$	100	100	100	100

[a] The pK_a for proton release in the high-pH pathway is 7 (0.8 proton); the pK_a for proton uptake, 11 (0.6 proton). For the uptake the rate of the reverse reaction was therefore negligible.

The rate constants used are given in Table I (for brevity, not all pH values used in the simulation are shown). Their values are consistent with earlier determined values (Váró & Lanyi, 1991c; Zimányi et al., 1992b, 1993). Importantly, we made pH dependent only the rates of the two protonation processes in the cycle: the reverse of the proton release on the extracellular side, in $M_1^{(-1)} \rightarrow M_1^{(0)}$, and the proton uptake on the cytoplasmic side in $N^{(-1)} \rightarrow N^{(0)}$ (at high pH) and $O^{(0)} \rightarrow O^{(+1)}$ (at low pH). For the sake of simplicity the rate constants in the low- and high-pH pathways were assumed to be the same. In this simulation the proton release on the extracellular side was associated with very rapid equilibration between two M_1 states, and its pK_a was 7. A similar result would have been obtained if the deprotonation had been associated with a rapid equilibrium between two M_2 states (Zimányi et al., 1992b). Since the pK_a for proton uptake on the cytoplasmic side is 11 (Zimányi et al., 1993), the rate of its reverse reaction was taken as insignificant. Earlier results suggested that the rate of the proton uptake is pH independent up to about 7, and above that it becomes pH dependent (Otto et al., 1989; Ames & Mathies, 1990; Zimányi et al., 1993). Figure 13 shows the amplitudes and time constants that resulted when the curves generated for M and O with these rate constants were analyzed as exponential processes in the same way as the measured data in Figure 11. It is evident that the model produces the same kind of phenomenological kinetic behavior as the measurements. The amplitudes of O and the slow decay component of M decline with pH (Figure 13). The amplitudes of the phenomenological M decay components are pH dependent in the way the $M \leftrightarrow N$ (or O) pathway predicts when the decay of $N^{(-1)}$ (or $O^{(0)}$) is pH dependent above pH 7 but not below. The decay of O follows the pH dependence of the time constant of the slower decay component of M because they are both affected by the proton uptake process on the cytoplasmic side: O is affected because the rate of accumulation of $O^{(+1)}$ depends on pH, and M is affected because it is in equilibrium with $N^{(-1)}$ or $O^{(0)}$ (Figures 10 and 12). Figures 11 and 13 illustrate, therefore, that with self-consistent rate constants, as in Table I, the model in Figure 12 will generate a photocycle that resembles the measured data.

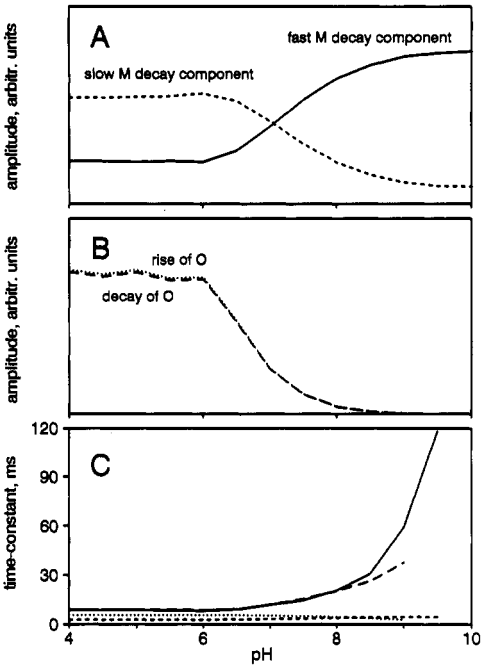

FIGURE 13: Simulated kinetics from the model in Figure 12. Kinetics for M and O were generated with the rate constants in Table I and treated like data as in Figure 11. Lines in panel C: (—) slow M decay component; (- - -) fast M decay component; (···) rise of O; (– –) decay of O.

DISCUSSION

It is to be expected that in a proton pump such as bacteriorhodopsin the identification and description of pH-dependent steps in the transport would yield mechanistic insights. In the functionally relevant range of pH 4–10 there are three conspicuous pH-dependent elements in the transport cycle: (1) the strong pH dependence of the time constant of the slow decay component for M at pH >8, (2) the reversal of the order of proton release and uptake below pH 6, and (3) the decrease of the amplitude of O (and increase in the amplitude of N) with increasing pH. The first of these is now understood to originate from the equilibration of a proton between the Schiff base and D96 and the subsequent pH-dependent proton uptake from the cytoplasmic surface (Otto et al., 1989; Ames & Mathies, 1990; Váró & Lanyi, 1991b; Druckmann et al., 1993; Zimányi et al., 1993). In this report we have explored the second and third effects and suggest that they are related to one another, both being influenced by the pH dependence for the course taken by the proton release

reaction in the protein. We have previously proposed a photocycle scheme that explained the pH dependence of the sequence of proton release and uptake (i.e., effect 2) with the participation of an extracellular proton release group XH in the transport when the pH is above its pK_a but not when it is below (Zimányi et al., 1992b). From the point of view of the proton transfers this meant that at the M_1 state the photocycle diverges into two pH-dependent alternative pathways (Figure 12). The present version of this model incorporates the additional feature that little or no N accumulates in the low-pH pathway and little or no O accumulates in the high-pH pathway. This would explain the reciprocal pH dependence for the amplitude of the O and N intermediates. Furthermore, the proton uptake occurs at low pH while the chromophore in the O state but at high pH while it is in the N state.

The events during the M to BR segment of the photocycle constitute the recovery of the initial state through reprotonation of the Schiff base from the cytoplasmic side and reestablishment of the all-trans isomeric state of the retinal. In order to understand the relationship of the proton uptake to the reisomerization, we need more detailed descriptions of the reactions that involve N and O. The model in Figure 12 suggests that in order to avoid the complication of multiple pathways O should be followed at low pH and N at high pH. Thus, we have examined the occurrence of proton uptake relative to the chromophore reactions in each of these pathways separately. In this report we concentrate on the events at low pH. Elsewhere, we describe the photocycle at high pH (Zimányi et al., 1993).

In the low-pH pathway the reisomerization of the retinal, as reflected in the rate of the N → O transition, appears to be more rapid than proton uptake. The accumulation of N is greatly diminished by its rapid decay. Proton uptake is after the rise but before the decay of O (Figure 8), which suggests the scheme $N^{(0)} \leftrightarrow O^{(0)} + H^+$ (from the bulk) $\leftrightarrow O^{(+1)} \rightarrow BR + H^+$ (to the bulk) as illustrated in Figure 10. Thus, the observed rise time of O is the rise time of $O^{(0)}$, and the decay of O is the decay of $O^{(+1)}$. The rise is not strongly pH dependent, and the decay becomes slower with increasing pH (Figure 11). The strong decline of the amplitude for O with increasing pH might reflect, therefore, the diminishing fraction of the photocycling bacteriorhodopsin passing through the low-pH pathway. We have found that in the high-pH pathway the order of reisomerization and proton uptake is the reverse of that at low pH (Zimányi et al., 1993). At high pH proton uptake is more rapid than the reisomerization, and as shown in Figure 10 the proposed scheme is $N^{(-1)} + H^+$ (from the bulk) $\leftrightarrow N^{(0)} \leftrightarrow O^{(0)} \rightarrow BR$.

Thus, the branching into the low- and high-pH pathways may be one of the factors that determines the relative rates for proton uptake and retinal isomerization. What are the influences on retinal isomerization that might be different in the two pathways? The chromophore reactions are the same at low and high pH, but in the low-pH pathway the extracellular proton release complex XH remains protonated throughout while in the high-pH pathway it deprotonates early in the photocycle (Figure 12). From the ionization states of D85, D212, R82 (or XH), and the Schiff base in the N intermediate, the net charge of the extracellular region of the protein is expected to be +1 at low pH but 0 at high pH. The increased rate of retinal isomerization at low pH in the N → O step might be influenced by this. Quantum chemical calculations (Warshel & Ottolenghi, 1979; Tavan et al., 1985) indicate that in a less electronegative environment for the Schiff base the barriers to isomerization of skeletal carbon–carbon bonds will be lowered. Balashov et al. (1992) suggested this kind of relationship between the protonation state of D85 and the thermal all-trans to 13-cis isomerization (dark-adaptation) rate from data for the rate of dark adaptation in the wild-type and R82A proteins. Replacement of D85 with asparagine resulted in a protein in which changing the pH in the dark produced M-, N-, and O-like states in thermal equilibrium (Turner et al., 1993). Reequilibration of these chromophore states upon changing the pH resulted in the unusually rapid reequilibration of the 13-cis and all-trans isomeric states of the retinal. Correlation of the rate of dark adaptation and the rate of reisomerization in the photocycle is supported by the phenotype of the T89A protein, which includes both very rapid dark adaptation and a greatly increased amount of O in the photocycle.[3] The increased positive charge in the low-pH pathway thus might have a similar consequence on the rate of reisomerization during the photocycle as removal of a negative charge in the unphotolyzed system. The properties of the R82Q mutant lend support to this possibility. The proton release complex is not functional in this system and the early proton release is absent (Otto et al., 1990; Balashov et al., 1992), but the net charge in the Schiff base region in N will be 0 rather than +1. Thus, although the proton kinetics of R82Q at neutral pH resemble those at low pH in wild type, rapid isomerization of the retinal in the photocycle and therefore the accumulation of large amounts of O are not expected. Indeed, the photocycle of R82Q (and of R82A, not shown) contains only very small amounts of the O state[4] (Balashov et al., 1992, and Figure 7).

According to the results we report here and elsewhere (Zimányi et al., 1992b, 1993), the chromophore cycle and the proton translocation are not fully coupled. The chromophore reactions are described by a single sequence, but the proton release step at M is optional and the subsequent proton-transfer reactions follow one of two different alternative pH-dependent pathways available for the transport. Simulation of this complex model produced a pattern of pH dependence for the absorption changes due to the M and O states similar to what is obtained experimentally. Since the transport of protons occurs over a wide pH range (from 4 to 10) which includes the pH where the cycle diverges, the two alternative proton transport pathways will occur with the same overall cytoplasmic-to-extracellular vectoriality.

[3] Brown, Needleman, and Lanyi, unpublished results.

[4] This is true even when the raised pK_a of D85 (that will have reduced the amount of purple chromophore at pH below 7) is taken into account.

REFERENCES

Ames, J. B., & Mathies, R. A. (1990) *Biochemistry 29*, 7181–7190.

Balashov, S., Govindjee, R., Kono, M., et al. (1992) in *Structures and Functions of Retinal Proteins* (Rigaud, J. L., Ed.) pp 111–114, John Libbey Eurotext Ltd., Montrouge, France.

Butt, H.- J., Fendler, K., Bamberg, E., Tittor, J., & Oesterhelt, D. (1989) *EMBO J. 8*, 1657–1663.

Cao, Y., Váró, G., Chang, M., Ni, B., Needleman, R., & Lanyi, J. K. (1991) *Biochemistry 30*, 10972–10979.

Cao, Y., Váró, G., Klinger, A. L., Czajkowsky, D. M., Braiman, M. S., Needleman, R., & Lanyi, J. K. (1993) *Biochemistry 32*, 1981–1990.

Chernavskii, D. S., Chizhov, I. V., Lozier, R. H., Murina, T. M., Prokhorov, A. M., & Zubov, B. V. (1989) *Photochem. Photobiol. 49*, 649–653.

Chizhov, I., Engelhard, M., Chernavskii, D. S., Zubov, B., & Hess, B. (1992) *Biophys. J. 61*, 1001–1006.

Dancsházy, Z., Govindjee, R., & Ebrey, T. G. (1988) *Proc. Natl. Acad. Sci. U.S.A. 85*, 6358–6361.
Dencher, N. A., & Wilms, M. (1975) *Biophys. Struct. Mech. 1*, 259–271.
Drachev, L. A., Kaulen, A. D., & Skulachev, V. P. (1984) *FEBS Lett. 178*, 331–335.
Druckmann, S., Heyn, M. P., Lanyi, J. K., Ottolenghi, M., & Zimányi, L. (1993) *Biophys. J.* (in press).
Ebrey, T. G. (1993) in *Thermodynamics of membranes, receptors and channels* (Jackson, M., Ed.) pp 353–387, CRC Press, New York.
Eisfeld, W., & Stockburger, M. (1992) in *Structures and Functions of Retinal Proteins* (Rigaud, J. L., Ed.) pp 139–142, John Libbey Eurotext Ltd., Montrouge, France.
Fodor, S. P., Ames, J. B., Gebhard, R., van der Berg, E. M., Stoeckenius, W., Lugtenburg, J., & Mathies, R. A. (1988) *Biochemistry 27*, 7097–7101.
Fukuda, K., & Kouyama, T. (1992) *Biochemistry 31*, 11740–11747.
Gerwert, K., Souvignier, G., & Hess, B. (1990) *Proc. Natl. Acad. Sci. U.S.A. 87*, 9774–9778.
Groma, G. I., Helgerson, S. L., Wolber, P. K., Beece, D., Dancsházy, Z., Keszthelyi, L. & Stoeckenius, W. (1984) *Biophys. J. 45*, 985–992.
Grzesiek, S., & Dencher, N. A. (1986) *FEBS Lett. 208*, 337–342.
Heberle, J., & Dencher, N. A. (1990) *FEBS Lett. 277*, 277–280.
Heberle, J., & Dencher, N. A. (1992) *Proc. Natl. Acad. Sci. U.S.A. 89*, 5996–6000.
Henderson, R., Baldwin, J. M., Ceska, T. A., Zemlin, F., Beckmann, E., & Downing, K. H. (1990) *J. Mol. Biol. 213*, 899–929.
Hoffmann, W., Graca-Miguel, M., Barnard, P., & Chapman, D. (1978) *FEBS Lett. 95*, 31–34.
Holz, M., Drachev, L. A., Mogi, T., Otto, H., Kaulen, A. D., Heyn, M. P., Skulachev, V. P., & Khorana, H. G. (1989) *Proc. Natl. Acad. Sci. U.S.A. 86*, 2167–2171.
Kouyama, T., Nasuda-Kouyama, A., Ikegami, A., Mathew, M. K., & Stoeckenius, W. (1988) *Biochemistry 27*, 5855–5863.
Lanyi, J. K. (1992) *J. Bioenerg. Biomembr. 24*, 169–179.
Lanyi, J. K., Tittor, J., Váró, G., Krippahl, G., & Oesterhelt, D. (1992) *Biochim. Biophys. Acta 1099*, 102–110.
Li, Q., Govindjee, R., & Ebrey, T. G. (1984) *Proc. Natl. Acad. Sci. U.S.A. 81*, 7079–7082.
Lozier, R. H., Niederberger, W., Ottolenghi, M., Sivorinovsky, G., & Stoeckenius, W. (1978) in *Energetics and Structure of Halophilic Microorganisms* (Caplan, S. R., & Ginzburg, M., Eds.) pp 123–139, Elsevier/North-Holland, Amsterdam.
Lozier, R. H., Xie, A., Hofrichter, J., & Clore, G. M. (1992) *Proc. Natl. Acad. Sci. U.S.A. 89*, 3610–3614.
Mathies, R. A., Lin, S. W., Ames, J. B., & Pollard, W. T. (1991) *Annu. Rev. Biophys. Biophys. Chem. 20*, 491–518.
Miller, A., & Oesterhelt, D. (1990) *Biochim. Biophys. Acta 1020*, 57–64.
Mogi, T., Stern, L. J., Marti, T., Chao, B. H., & Khorana, H. G. (1988) *Proc. Natl. Acad. Sci. U.S.A. 85*, 4148–4152.
Needleman, R., Chang, M., Ni, B., Váró, G., Fornes, J., White, S. H., & Lanyi, J. K. (1991) *J. Biol. Chem. 266*, 11478–11484.
Ni, B., Chang, M., Duschl, A., Lanyi, J. K., & Needleman, R. (1990) *Gene 90*, 169–172.
Oesterhelt, D., & Stoeckenius, W. (1974) *Methods Enzymol. 31*, 667–678.
Oesterhelt, D., Tittor, J., & Bamberg, E. (1992) *J. Bioenerg. Biomembr. 24*, 181–191.
Ohtani, H., Kobayashi, T., Iwai, J.-I., & Ikegami, A. (1986) *Biochemistry 25*, 3356–3363.
Ohtani, H., Itoh, H., & Shinmura, T. (1992) *FEBS Lett. 305*, 6–8.
Otto, H., Marti, T., Holz, M., Mogi, T., Lindau, M., Khorana, H. G., & Heyn, M. P. (1989) *Proc. Natl. Acad. Sci. U.S.A. 86*, 9228–9232.
Otto, H., Marti, T., Holz, M., Mogi, T., Stern, L. J., Engel, F., Khorana, H. G., & Heyn, M. P. (1990) *Proc. Natl. Acad. Sci. U.S.A. 87*, 1018–1022.
Scherrer, P., Alexiev, U., Otto, H., Heyn, M. P., Marti, T., & Khorana, H. G. (1992) in *Structures and Functions of Retinal Proteins* (Rigaud, J. L., Ed.) pp 205–211, John Libbey Eurotext Ltd., Montrouge, France.
Sherman, W. V., Eicke, R. R., Stafford, S. R., & Wasacz, F. M. (1979) *Photochem. Photobiol. 30*, 727–729.
Smith, S. O., Pardoen, J. A., Mulder, P. P. J., Curry, B., Lugtenburg, J., & Mathies, R. A. (1983) *Biochemistry 22*, 6141–6148.
Souvignier, G., & Gerwert, K. (1992) *Biophys. J. 63*, 1393–1405.
Stern, L. J., Ahl, P. L., Marti, T., Mogi, T., Duñach, M., Berkovitz, S., Rothschild, K. J., & Khorana, H. G. (1989) *Biochemistry 28*, 10035–10042.
Subramaniam, S., Marti, T., & Khorana, H. G. (1990) *Proc. Natl. Acad. Sci. U.S.A. 87*, 1013–1017.
Subramaniam, S., Greenhalgh, D. A., Rath, P., Rothschild, K. J., & Khorana, H. G. (1991) *Proc. Natl. Acad. Sci. U.S.A. 88*, 6873–6877.
Subramaniam, S., Greenhalgh, D. A., & Khorana, H. G. (1992) *J. Biol. Chem. 267*, 25730–25733.
Tavan, P., Schulten, K., & Oesterhelt, D. (1985) *Biophys. J. 47*, 415–430.
Thorgeirsson, T. E., Milder, S. J., Miercke, L. J. W., Betlach, M. C., Shand, R. F., Stroud, R. M., & Kliger, D. S. (1991) *Biochemistry 30*, 9133–9142.
Turner, G. J., Miercke, L. J. W., Thorgeirsson, T. E., Kliger, D. S., Betlach, M. C., & Stroud, R. M. (1993) *Biochemistry 32*, 1332–1337.
Váró, G., & Lanyi, J. K. (1990) *Biochemistry 29*, 2241–2250.
Váró, G., & Lanyi, J. K. (1991a) *Biophys. J. 59*, 313–322.
Váró, G., & Lanyi, J. K. (1991b) *Biochemistry 30*, 5016–5022.
Váró, G., & Lanyi, J. K. (1991c) *Biochemistry 30*, 5008–5015.
Váró, G., Duschl, A., & Lanyi, J. K. (1990) *Biochemistry 29*, 3798–3804.
Warshel, A., & Ottolenghi, M. (1979) *Photochem. Photobiol. 30*, 291–293.
Zimányi, L., Cao, Y., Chang, M., Ni, B., Needleman, R., & Lanyi, J. K. (1992a) *Photochem. Photobiol. 56*, 1049–1055.
Zimányi, L., Váró, G., Chang, M., Ni, B., Needleman, R., & Lanyi, J. K. (1992b) *Biochemistry 31*, 8535–8543.
Zimányi, L., Cao, Y., Needleman, R., Ottolenghi, M., & Lanyi, J. K. (1993) *Biochemistry 32*, 7669–7678.